

Technical Notes

TECHNICAL NOTES are short manuscripts describing new developments or important results of a preliminary nature. These Notes should not exceed 2500 words (where a figure or table counts as 200 words). Following informal review by the Editors, they may be published within a few months of the date of receipt. Style requirements are the same as for regular contributions (see inside back cover).

Energy Deposition/Absorption Effects on a Planar Shock Wave

Chunpei Cai*

ZONA Technology, Inc., Scottsdale, Arizona 85258

DOI: 10.2514/1.27970

Nomenclature

e	=	inner energy
L	=	energy deposition/absorption zone length
M	=	Mach number
p	=	pressure
p_0	=	total pressure
\dot{Q}, q	=	energy deposition/absorption strength
R	=	universal gas constant
T	=	temperature
u	=	velocity
γ	=	specific heat ratio, 1.4
ρ	=	density
σ	=	deposition/absorption strength parameter, $L\dot{Q}/(RT_1\sqrt{\gamma RT_1})$

Subscripts

1	=	preenergy deposition/absorption state
2	=	postenergy deposition/absorption state
3	=	postshock state

I. Introduction

ENERGY deposition for modification of the external flowfield around a vehicle is a well-known technique and has been studied and used to reduce the drag on the objects flying at supersonic speeds. Since the 1950s, energy deposition in the supersonic flow was proposed as an alternative technique to reduce drag on flying objects [1,2]. Many papers discuss the significant drag decrease by energy deposition in front of an object. Analytical, numerical, and experimental studies were reported [3–11].

Many energy deposition applications share the same flowfield structure: in front of a shock wave, energy is deposited and results in large pressure changes behind the shock wave. This note aims to analytically study a simplified, yet related, one-dimensional problem, which is shown in Fig. 1. In front of a stationary planar normal shock wave, there is a region (with length L) in which energy is deposited or absorbed. There are three regions in the flowfield: the predeposition region 1, the preshock and postdeposition region 2, and the postshock region 3. Between regions 1 and 2, energy is deposited/absorbed with a strength of $\rho\dot{Q}$. The properties in each

region can be considered constant. This note aims to obtain the preshock energy deposition/absorption effects on the postshock properties. This problem has applications in external flows, such as the drag reduction for flying objects, and in internal flows, such as supersonic, heated/cooled gas into a combustor.

II. Analytical Solutions and Discussions

With an aim to obtain analytical solutions, we select the Euler equations and neglect the gas viscosity and thermal conductivity. The one-dimensional governing equations with energy deposition/absorption are [12]

$$p = \rho RT \quad (1)$$

$$\frac{\partial \rho}{\partial t} + \frac{\partial(\rho u)}{\partial x} = 0 \quad (2)$$

$$\frac{\partial(\rho u)}{\partial t} + \frac{\partial(p + \rho u^2)}{\partial x} = 0 \quad (3)$$

$$\frac{\partial(e)}{\partial t} + \frac{\partial(pu + eu)}{\partial x} = \rho \dot{q} \quad (4)$$

The inner energy has the following relation with respect to the other variables: $e = p/(\gamma - 1) + \rho u^2/2$. Note, as stated earlier, the right-hand side of Eq. (4) is zero everywhere in the flowfield, except between regions 1 and 2, where it has a constant value of $\rho\dot{Q}$.

For a steady flow with a stationary planar shock wave, the preceding equations reduce to simple algebraic relations. Especially, the energy equation can be simplified as

$$\begin{aligned} \frac{\gamma}{\gamma - 1} p_1 u_1 + \frac{1}{2} \rho_1 u_1^3 + \rho_1 \dot{Q} L &= \frac{\gamma}{\gamma - 1} p_2 u_2 + \frac{1}{2} \rho_2 u_2^3 \\ &= \frac{\gamma}{\gamma - 1} p_3 u_3 + \frac{1}{2} \rho_3 u_3^3 \end{aligned}$$

with an assumption that across the deposition/absorption layer, the density maintains a constant of ρ_1 .

We define a nondimensional parameter $\sigma = L\dot{Q}/(RT_1\sqrt{\gamma RT_1})$ to represent the energy deposition/absorption strength. Then, from the algebraic relations, the following simple relation between ρ_1 and ρ_2 exists:

$$\begin{aligned} \frac{\gamma + 1}{2(\gamma - 1)} \gamma M_1^2 \left(\frac{\rho_1}{\rho_2} \right)^2 - \left(\frac{\gamma}{\gamma - 1} + \frac{\gamma^2 M^2}{\gamma - 1} \right) \frac{\rho_1}{\rho_2} + \left(\frac{\gamma}{\gamma - 1} + \frac{\gamma M_1^2}{2} \right. \\ \left. + \frac{\sigma}{M_1} \right) = 0 \end{aligned} \quad (5)$$

With the compatible relation that $\rho_1 = \rho_2$ without any energy deposition and absorption, the following root of Eq. (5) is the correct relation between ρ_1 and ρ_2 :

Received 22 September 2006; accepted for publication 29 September 2006. Copyright © 2006 by the American Institute of Aeronautics and Astronautics, Inc. All rights reserved. Copies of this paper may be made for personal or internal use, on condition that the copier pay the \$10.00 per-copy fee to the Copyright Clearance Center, Inc., 222 Rosewood Drive, Danvers, MA 01923; include the code \$10.00 in correspondence with the CCC.

*CFD Specialist, 9489 East Ironwood Square Drive. Member AIAA.

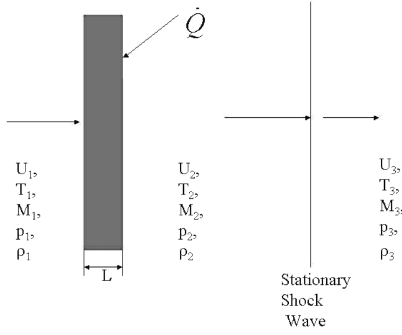


Fig. 1 Illustration of the flow problem.

$$\frac{\rho_1}{\rho_2} = \frac{\gamma + \gamma^2 M_1^2 + A}{(\gamma + 1) \gamma M_1^2} \quad (6)$$

where

A

$$= \sqrt{(\gamma + \gamma^2 M_1^2)^2 - 2(\gamma/(\gamma - 1) + \gamma M_1^2/2 + \sigma/M_1)(\gamma^2 - 1)\gamma M_1^2}$$

The other relations between regions 1 and 2 are

$$\frac{p_2}{p_1} = \frac{\gamma M_1^2 + 1 - A}{\gamma + 1} \quad (7)$$

$$\frac{T_2}{T_1} = \frac{p_2 \rho_1}{p_1 \rho_2} = \frac{(\gamma + \gamma^2 M_1^2 + A)(\gamma M_1^2 + 1 - A)}{(\gamma + 1) \gamma M_1^2} \quad (8)$$

$$\frac{M_2^2}{M_1^2} = \frac{\rho_1 p_1}{\rho_2 p_2} = \frac{[\gamma + \gamma^2 M_1^2 + A]}{[\gamma M_1^2][\gamma M_1^2 + 1 - A]} \quad (9)$$

It can be shown that the energy deposition or absorption cannot be infinitely strong; on one limit, A needs to be a real number, and on the other limit, p_2 should be greater than zero. With these two relations, the following relation can be obtained:

$$\sigma_{\min} = \frac{\gamma - 1 - 2\gamma M_1^2}{2(\gamma - 1)\gamma M_1} < \sigma < \frac{\gamma(M_1^2 - 1)^2}{2M_1(\gamma^2 - 1)} = \sigma_{\max} \quad (10)$$

Note that the scope of energy deposition is much wider than that for energy absorption with $\sigma_{\max} > |\sigma_{\min}|$; when $\sigma = 0$, regions 1 and 2 have the same properties, whereas with the maximum energy deposition, $\rho_2/\rho_1 = (\gamma + 1)M_1^2/(1 + \gamma M_1^2)$, $p_2/p_1 = (\gamma M_1^2 + 1)/(\gamma + 1)$, $T_2/T_1 = (1 + \gamma M_1^2)^2/[(\gamma + 1)^2 M_1^2]$, and $M_2 = 1$. The maximum energy deposition value is little different from Georgievskii and Levin's [4] previous result, because the definition of σ was different, and a Gaussian distribution for the energy deposition, extending to an infinite distance in front of the shock wave, was assumed in their paper. Equation (10) indicates there is a critical value for the energy absorption situation, as well.

Note that all properties across the deposition/absorption layer are completely determined by the nondimensional parameter σ and the incoming Mach number. When the incoming Mach number becomes large, the postdeposition effects diminish.

With the deposition/absorption strength properly bounded, we can further compare its effect on the postshock properties, which is the major purpose of this note. From region 2 to region 3, the classical Rankine-Hugoniot relations hold, which can be found in many aerodynamics books [13]. The final relations between regions 3 and 1 are

$$\frac{p_3}{p_1} = \left[\frac{2\gamma M_2^2 - (\gamma - 1)}{\gamma + 1} \right] \left[\frac{\gamma M_1^2 + 1 - A}{\gamma + 1} \right] \quad (11)$$

$$\frac{u_3}{u_1} = \frac{\rho_1}{\rho_3} = \frac{\gamma + \gamma^2 M_1^2 + A}{(\gamma + 1)\gamma M_1^2} \left[\frac{2 + (\gamma - 1)M_2^2}{(\gamma + 1)M_2^2} \right] \quad (12)$$

$$\frac{T_3}{T_1} = \left(\frac{[2\gamma M_2^2 - (\gamma - 1)][2 + (\gamma - 1)M_2^2]}{(\gamma + 1)^2 M_2^2} \right) \times \left(\frac{(\gamma + \gamma^2 M_1^2 + A)(\gamma M_1^2 + 1 - A)}{(\gamma + 1)\gamma M_1^2} \right) \quad (13)$$

$$\frac{p_{03}}{p_{01}} = \frac{[(\gamma + 1)M_2^2]^{\gamma/(\gamma-1)}}{[\frac{2\gamma M_2^2 - (\gamma-1)}{(\gamma+1)}]^{1/(\gamma-1)}} \frac{1}{(2 + (\gamma - 1)M_1^2)^{\gamma/(\gamma-1)}} \times \left(\frac{\gamma M_1^2 + 1 - A}{\gamma + 1} \right) \quad (14)$$

To discuss these analytical results, the preshock and postshock conditions vs the deposition/absorption strength are plotted with an incoming Mach number $M_1 = 10.0$ and $\gamma = 1.4$.

Figure 2 shows the energy deposition/absorption effects on the preshock and postshock Mach numbers and densities. When the deposition strength increases, the preshock density increases and the Mach number rapidly decreases, resulting in a weaker shock wave. When the deposition reaches its maximum value, the shock ceases to exist, and this maximum deposition value is a critical point. On the other hand, stronger absorption will decrease the preshock density and increase the Mach number in front of the shock. At the absorption limit, an infinitely large preshock Mach number is created and the postshock density reaches the hypersonic limit of six.

Figure 3 shows the deposition/absorption effects on the static temperatures and postshock stagnation temperature. As the

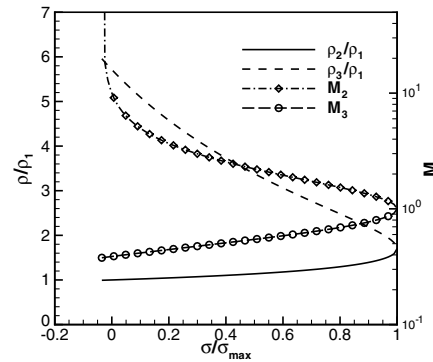


Fig. 2 Energy deposition/absorption effects on Mach number and density results; $M_1 = 10.0$ and $\gamma = 1.4$.

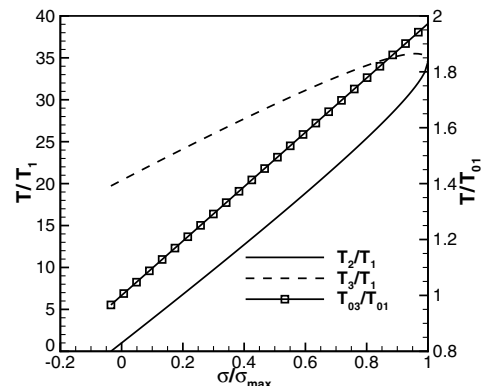


Fig. 3 Energy deposition/absorption effects on temperature results; $M_1 = 10.0$ and $\gamma = 1.4$.

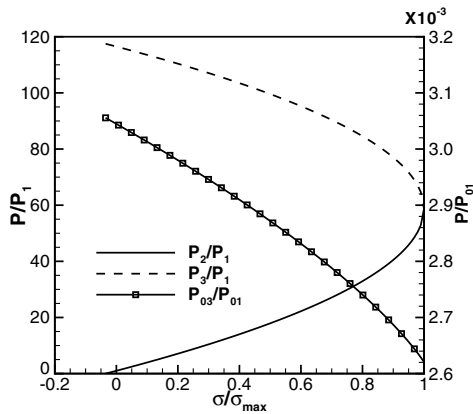


Fig. 4 Energy deposition/absorption effects on pressure results; $M_1 = 10.0$ and $\gamma = 1.4$.

deposition increases, all the temperatures continue to increase; although continuing energy absorption eventually results in a zero static preshock temperature.

Figure 4 shows that stronger energy deposition results in a higher postshock pressure, but lower postshock static and stagnation pressure; although energy absorption will result in higher postshock static and stagnant pressure. We can conclude that if an object exists behind the shock, the heat deposition in front of a shock reduces the wave drag.

III. Conclusions

In this study, we analyzed the effects of energy deposition and absorption on the postshock properties. With Euler Equations, simple algebraic relations exist among the three regions. The results indicate that energy depositions increase the gas density in the postdeposition region and result in lower preshock Mach numbers, and with the critical energy deposition value, the shock ceases to exist. Stronger energy absorption in front of the shock increases the preshock Mach number. Overall, energy depositions result in higher postshock temperature, lower density, and lower static/stagnation pressure, whereas energy absorption yields the exact opposite effects.

Acknowledgments

This work is partially supported by the independent research and development funding from ZONA Technology, Inc., and the author would like to thank Quanhua Sun for discussions.

References

- [1] Oswatich, K., "Propulsion with Heating at Supersonic Speed," Deutsche Versuchsanstalt fuer Luft und Raumfahrt, Rept. 90, 1959.
- [2] Pinkel, I. L., Serafini, J. S., and Gregg, J. L., "Pressure Distribution and Aerodynamic Coefficients Associated with Heat Addition to Supersonic Air Stream Adjacent to Two-Dimensional Supersonic Wing," NACA Rept. RM E51K26, 1952.
- [3] Shneider, M. N., Macheret, S. O., Zaidi, S. H., Girgis, I. G., Raizer, Yu. P., and Miles, R. B., "Steady and Unsteady Supersonic Flow Control with Energy Addition," 34th AIAA Plasmadynamics and Lasers Conference, Orlando, FL, AIAA Paper 2003-3862, June 2003.
- [4] Georgievskii, P. Yu., and Levin, V. A., "Control of the Flow Past Bodies Using Localized Energy Addition to the Supersonic Oncoming Flow," *Fluid Dynamics*, Vol. 38, No. 5, 2003, pp. 794–805.
- [5] Riggins, D., Nelson, H. F., and Johnson, E., "Blunt-Body Wave Drag Reduction Using Focused Energy Deposition," *AIAA Journal*, Vol. 37, No. 4, 1999, pp. 406–467.
- [6] Myrabo, L. N., and Raizer, Yu. P., "Laser-Induced Air Spike for Advanced Transatmospheric Vehicles," 25th Plasmadynamics and Laser Conference, Colorado Springs, CO, AIAA Paper 94-2551, 1994.
- [7] Kandala, R., and Candler, G., "Numerical Studies of Laser-Induced Energy Deposition for Supersonic Flow Control," 41st Aerospace Sciences Meeting and Exhibit, Reno, NV, AIAA Paper 2003-1052, Jan. 6–9th, 2003.
- [8] Yan, H., Adlgren, R., Elliott, G., Knight, D., Beuther, T., and Ivanov, M., "Laser Energy Deposition in Intersecting Shocks," 1st Flow Control Conference, St. Louis, MO, AIAA Paper 2002-2729, 2002.
- [9] Kremeyer, K., Sebastian, K., and Shu, C. W., "Computational Study of Shock Mitigation and Drag Reduction by Pulsed Energy Lines," *AIAA Journal*, Vol. 44, No. 8, Aug. 2006, pp. 1720–1731.
- [10] Ganiev, Y. C., Gordeev, V. P., Krasilnikov, A. V., Lagutin, V. I., Otmennikov, V. N., and Panasenko, A. V., "Aerodynamic Drag Reduction by Plasma and Hot-Gas Injection," *AIAA Journal*, Vol. 14, No. 1, Jan.–Mar. 2000, pp. 10–17.
- [11] Latypov, A. F., and Fomin, V. M., "Evaluation of the Energy Efficiency of Heat Addition Upstream of the Body in a Supersonic Flow," *Journal of Applied Mechanics and Technical Physics*, Vol. 43, No. 1, 2002, pp. 59–62.
- [12] Zel'dovich, Ya. B., and Raizer, Yu. P., *Physics of Shock Waves and High-Temperature Hydrodynamic Phenomena*, edited by W. D. Hayes and R. F. Probstein, Dover, Mineola, NY, 2002.
- [13] Saad, M. A., *Compressible Fluid Flow*, Prentice-Hall, Upper Saddle River, NJ, 1993.